

# Excluded-Volume Effects on the Hydrodynamic Radius of Atactic and Isotactic Oligo- and Poly(methyl methacrylate)s in Dilute Solution

Toshihiro Arai, Nobuo Sawatari, Takenao Yoshizaki,  
Yoshiyuki Einaga, and Hiromi Yamakawa\*

Department of Polymer Chemistry, Kyoto University, Kyoto 606-01, Japan

Received August 29, 1995; Revised Manuscript Received November 20, 1995<sup>⊗</sup>

**ABSTRACT:** The translational diffusion coefficient  $D$  was determined from dynamic light scattering measurements for atactic (a-) and isotactic (i-) oligo- and poly(methyl methacrylate)s (PMMA) in acetone at 25.0 °C in the range of weight-average molecular weight  $M_w$  from  $1.83 \times 10^3$  to  $9.52 \times 10^5$  for the former and from  $3.04 \times 10^3$  to  $9.78 \times 10^5$  for the latter. For each PMMA, the values of the (perturbed) hydrodynamic radius  $R_H$  (defined from  $D$ ) in acetone were found to agree with those of the radius  $R_{H,\Theta}$  previously (and presently) obtained in the unperturbed ( $\Theta$ ) state (i.e., in acetonitrile at 44.0 °C for a-PMMA and at 28.0 °C for i-PMMA) in the oligomer region. The hydrodynamic-radius expansion factor  $\alpha_H$  was then determined correctly from the values of  $R_H$  and  $R_{H,\Theta}$ . The results for  $\alpha_H$  as a function of the scaled excluded-volume parameter  $\tilde{z}$  defined in the Yamakawa–Stockmayer–Shimada theory for the helical wormlike chain with excluded volume are consistent with the previous results for atactic polystyrene, poly(dimethylsiloxane), and polyisobutylene. This leads to the conclusion that the quasi-two-parameter scheme may be valid for  $\alpha_H$  as well as for the gyration-radius and viscosity-radius expansion factors  $\alpha_S$  and  $\alpha_\eta$  irrespective of the large differences in chain stiffness, local conformation, and solvent condition. It is again found that the Barrett equation overestimates  $\alpha_H$ . This disagreement between theory and experiment may be explained only semiquantitatively by the Yamakawa–Yoshizaki theory, which takes account of the possible effect of fluctuating hydrodynamic interaction on  $\alpha_H$ . This indicates that it requires further theoretical investigations. It is also again found that  $\alpha_H$  coincides with  $\alpha_\eta$  within experimental error over the whole range of  $M_w$  studied.

## Introduction

In the preceding paper,<sup>1</sup> we have made a study of the hydrodynamic-radius expansion factor  $\alpha_H$  for polyisobutylene (PIB) as a part of this series of experimental work on the excluded-volume effects in dilute solutions of oligomers and polymers.<sup>2</sup> The validity of the quasi-two-parameter (QTP) scheme for  $\alpha_H$  as well as for the gyration-radius and viscosity-radius expansion factors  $\alpha_S$  and  $\alpha_\eta$  was confirmed; i.e., these factors may be expressed as functions only of the scaled excluded-volume parameter  $\tilde{z}$  defined in the Yamakawa–Stockmayer–Shimada (YSS) theory<sup>3–5</sup> that takes account of the effects of excluded volume and chain stiffness on the basis of the helical wormlike (HW) chain model,<sup>6,7</sup> irrespective of the polymer–solvent system. In this paper, we make a similar study of  $\alpha_H$  for atactic poly(methyl methacrylate) (a-PMMA) with the fraction of racemic diads  $f_r = 0.79$  and also for isotactic (i-) PMMA with  $f_r \approx 0.01$  for the further confirmation of that validity.

Now, within the framework of the application of the HW chain model, the a-PMMA chain has the largest chain stiffness  $\lambda^{-1}$  and the strongest *helical nature*<sup>8,9</sup> of all flexible polymers we have studied so far,<sup>9,10</sup> having the characteristic local conformation such that it retains large helical portions in dilute solution. On the other hand, the i-PMMA chain is rather like atactic polystyrene (a-PS); it has a much smaller chain stiffness and weaker helical nature than the a-PMMA chain because of the large difference between their values of  $f_r$ , thus leading to the remarkable difference between them in dilute solution behavior.<sup>9</sup> Thus the previous results for  $\alpha_S$  and  $\alpha_\eta$  for a-PMMA<sup>12</sup> and i-PMMA<sup>13</sup> may be consid-

ered a strong support to the validity of the QTP scheme above for these factors. This may also be expected for their  $\alpha_H$ .

Following the newly established guideline in this series of papers on the excluded-volume effects, we have already confirmed that the unperturbed values  $\langle S^2 \rangle_\Theta$  of the mean-square radius of gyration for a-PMMA<sup>12</sup> in acetonitrile at 44.0 °C ( $\Theta$ ) and for i-PMMA<sup>13</sup> in acetonitrile at 28.0 °C ( $\Theta$ ) coincide with the respective values  $\langle S^2 \rangle$  in their good solvent acetone at 25.0 °C in the oligomer region. Then the values of  $\alpha_S$  for the two PMMAs in acetone have been able to be calculated by adopting the respective  $\langle S^2 \rangle_\Theta$  in acetonitrile as the corresponding unperturbed values  $\langle S^2 \rangle_0$  in acetone.

In the case of  $\alpha_\eta$ , the situation is somewhat complicated because of the dependence on solvent of the Flory–Fox factor  $\Phi_\infty$  (in the coil limit).<sup>12–15</sup> Specifically, the values of the intrinsic viscosity  $[\eta]$  for the a-PMMA oligomer samples in acetone are larger than those of  $[\eta]_\Theta$  in acetonitrile at  $\Theta$  and rather agree with those of  $[\eta]_\Theta$  in another  $\Theta$  solvent *n*-butyl chloride at 40.8 °C.<sup>12</sup> This is the case with i-PMMA,<sup>13</sup> although  $[\eta]_\Theta$  have not been determined in *n*-butyl chloride. Then, in order to make a correction for this effect in the calculation of  $\alpha_\eta$ , the coefficient  $C_\eta$  has been introduced and appropriately determined.<sup>12,13</sup> Fortunately, however, such a difficulty does not occur in the determination of  $\alpha_H$ . The reason for this is that the values of the hydrodynamic radius  $R_{H,\Theta}$  (and also  $\langle S^2 \rangle_\Theta$ ) for a-PMMA in acetonitrile at  $\Theta$  and in *n*-butyl chloride at  $\Theta$  have been found to agree with each other within experimental error over the whole range of the molecular weight studied,<sup>16</sup> so that the difference between the values of the transport factor  $\rho_\infty$  (in the coil limit) in the two  $\Theta$  solvents is negligibly small if any. Thus, in the present paper, we use acetone and acetonitrile as good and  $\Theta$

<sup>⊗</sup> Abstract published in *Advance ACS Abstracts*, February 15, 1996.

**Table 1. Values of  $M_w$ ,  $x_w$ , and  $M_w/M_n$  for Atactic Oligo- and Poly(methyl methacrylate)s**

sample	$M_w$	$x_w$	$M_w/M_n$
OM18a <sup>a</sup>	$1.83 \times 10^3$	18.3	1.05
OM42	$4.18 \times 10^3$	41.8	1.09
OM76	$7.55 \times 10^3$	75.5	1.08
MM2a	$2.02 \times 10^4$	202	1.08
MM5	$5.04 \times 10^4$	504	1.07
MM7 <sup>b</sup>	$7.40 \times 10^4$	740	1.09
MM12	$1.19 \times 10^5$	1190	1.09
MM20	$2.04 \times 10^5$	2040	1.08
MM31	$3.12 \times 10^5$	3120	1.08
Mr5	$4.82 \times 10^5$	4820	1.07
Mr10	$9.52 \times 10^5$	9520	1.07

<sup>a</sup>  $M_w$ s of OM18a through Mr5 had been determined from SLS in acetone at 25.0 °C except for MM7 and MM12.<sup>12</sup> <sup>b</sup>  $M_w$ s of MM7 and MM12 had been determined from SLS in acetonitrile at 44.0 °C.<sup>11</sup>

**Table 2. Values of  $M_w$ ,  $x_w$ , and  $M_w/M_n$  for Isotactic Oligo- and Poly(methyl methacrylate)s**

sample	$M_w$	$x_w$	$M_w/M_n$
iOM31 <sup>a</sup>	$3.04 \times 10^3$	29.8	1.07
iOM71	$7.27 \times 10^3$	72.1	1.05
iMM3	$3.09 \times 10^4$	308	1.06
iMMc7 <sup>b</sup>	$7.01 \times 10^4$	700	1.06
iMMc16	$1.54 \times 10^5$	1540	1.08
iMMc40	$3.79 \times 10^5$	3790	1.06
iMMc70	$6.86 \times 10^5$	6860	1.06
iMMc90	$9.78 \times 10^5$	9780	1.09

<sup>a</sup>  $M_w$ s of iOM31 through iMMc90 had been determined from SLS in acetone at 25.0 °C except for iMMc7.<sup>13,24</sup> <sup>b</sup>  $M_w$ s of iMMc7 had been determined from SLS in acetonitrile at 28.0 °C.<sup>17</sup>

solvents, respectively, to determine  $\alpha_H$  without any correction like  $C_\eta$ .

## Experimental Section

**Materials.** Most of the a- and i-PMMA samples used in this work are the same as those used in the previous studies of  $\langle S^2 \rangle$ ,<sup>9,11</sup>  $\langle S^2 \rangle$ ,<sup>12,13</sup>  $[\eta]$ ,<sup>14,17</sup>  $[\eta]$ ,<sup>12,13</sup>  $D_0$ ,<sup>16,17</sup> the mean-square optical anisotropy  $\langle \Gamma^2 \rangle$ ,<sup>18,19</sup> the scattering function  $P(k)$ ,<sup>20,21</sup> the second virial coefficient  $A_2$ ,<sup>22–24</sup> and the dynamic depolarized light scattering component  $J_T$ .<sup>25</sup>

The a-PMMA samples are the fractions separated by preparative gel permeation chromatography (GPC) or fractional precipitation from the original samples prepared by group-transfer polymerization for the weight-average molecular weight  $M_w < 4 \times 10^5$  and by radical polymerization for  $M_w > 4 \times 10^5$ . In this work, one additional sample was prepared by fractional precipitation from the latter original sample using benzene as a solvent and methanol as a precipitant as before.<sup>9</sup> All the a-PMMA samples have a fixed stereochemical composition (the fraction of racemic diads  $f_r = 0.79$ ) independent of  $M_w$ , possessing hydrogen atoms at both ends of the chain. The values of  $M_w$ , the weight-average degree of polymerization  $x_w$  calculated from  $M_w$ , and the ratio of  $M_w$  to the number-average molecular weight  $M_n$  determined by analytical GPC are listed in Table 1. The sample Mr10 is an additional one and its  $M_w$  was determined from static light scattering (SLS) measurements in acetone at 25.0 °C (see below). The values of  $M_w/M_n$  indicate that the molecular weight distributions of all the samples are sufficiently narrow for the present purpose.

The i-PMMA samples are the fractions separated by preparative GPC or fractional precipitation from the original samples prepared by living anionic polymerization or from the commercial sample 9011-14-7 from Scientific Polymer Products, Inc. The synthesized samples have a *tert*-butyl group at the initiating chain end and a hydrogen atom at the other end. All the i-PMMA samples have a fixed stereochemical composition ( $f_r \approx 0.01$ ) independent of  $M_w$ . The values of  $M_w$ ,  $x_w$ , and  $M_w/M_n$  are listed in Table 2. It is seen that all these samples are also sufficiently narrow in molecular weight distribution.

The solvents acetone and acetonitrile used for dynamic light scattering (DLS), SLS, and viscosity measurements were purified according to standard procedures.

**Dynamic Light Scattering.** DLS measurements were carried out to determine  $D$  for all the a- and i-PMMA samples in acetone at 25.0 °C, and also  $D_0$  for seven a-PMMA samples in acetonitrile at 44.0 °C ( $\Theta$ ) and for two i-PMMA samples in acetonitrile at 28.0 °C ( $\Theta$ ). We had already determined  $D_0$  for the other samples and also the a-PMMA sample MM2a in the previous studies.<sup>16,17</sup> As for this sample, we redetermined  $D_0$  since the accuracy of the previous result<sup>16</sup> did not seem good enough for the present purpose.

The apparatus system, experimental procedure, and method of data analysis are the same as those described in the preceding paper<sup>1</sup> except the following data acquisition procedure for the measurements of the normalized autocorrelation function  $g^{(2)}(t)$  of the scattered light intensity  $I(t)$  at time  $t$ . For solutions of a- and i-PMMA, some effects of residual aggregates of solute molecules on  $g^{(2)}(t)$  had been observed in the previous studies,<sup>16,17</sup> so that it was measured again by the use of the data acquisition procedure introduced therein<sup>16</sup> in order to remove the effects. In principle, the procedure consists of measuring successively a large number of sets of 264 values of  $g^{(2)}(j\tau)$  with  $\tau$  the sampling time ( $j = 1, 2, \dots, 264$ ), the measurement for each set being made during 20 s. Only those sets of values which are free of such effects are then accumulated.

The quantity  $g^{(2)}(t)$  was measured at four or five concentrations and at scattering angles ranging from 20 to 50°. The most concentrated solutions of each sample were prepared gravimetrically and made homogeneous by continuous stirring at ca. 50 °C for ca. 1 day in acetone and for ca. 3 days in acetonitrile, preventing the solutions from being exposed to light. They were optically purified by filtration through a Teflon membrane of pore size 0.45 or 0.10  $\mu\text{m}$ . The solutions of lower concentrations were obtained by successive dilution. The polymer mass concentrations  $c$  were calculated from the weight fractions with the densities of the solutions.

The values of the refractive index at 488 nm and the viscosity coefficient  $\eta_0$  used are 1.361 and 0.306 cP, respectively, for acetone at 25.0 °C, 1.337 and 0.285 cP, respectively, for acetonitrile at 44.0 °C, and 1.344 and 0.331 cP, respectively, for acetonitrile at 28.0 °C. We note that  $\eta_0$  of acetone was measured with a capillary viscometer using pure cyclohexane as a reference, for which the literature value is available.

**Static Light Scattering.** SLS measurements were carried out to determine  $\langle S^2 \rangle$  (and also  $M_w$ ) for the additional a-PMMA sample Mr10 in acetone at 25.0 °C and in acetonitrile at 44.0 °C ( $\Theta$ ). The apparatus system, experimental procedure, and method of data analysis are the same as those described in the previous papers.<sup>11,12</sup>

**Viscosity.** Viscosity measurements were also carried out for the samples Mr10 and iMMc7 in acetone at 25.0 °C and for the sample Mr10 in acetonitrile at 44.0 °C ( $\Theta$ ) in order to evaluate  $\alpha_\eta$  for them in acetone at 25.0 °C. The test solutions were prepared in the same manner as in the case of DLS measurements. The apparatus system, experimental procedure, and method of data analysis are the same as those described in the preceding paper.<sup>1</sup>

## Results

**Translational Diffusion Coefficient.** Figures 1 and 2 show plots of the apparent diffusion coefficient<sup>1,10</sup>  $D^{(LS)}(c)$  against  $c$  for all the samples of a- and i-PMMA, respectively, examined in acetone at 25.0 °C. (We have omitted the plots for a- and i-PMMA in acetonitrile at the respective  $\Theta$ s, since they are similar to those shown in refs 16 and 17, respectively.) The data points for each sample are seen to follow a straight line, and thus  $D^{(LS)}(0)$  ( $=D$ ) and  $k_D^{(LS)}$  defined by eq 4 of ref 1 may be accurately determined from its ordinate intercept and slope, respectively. It is also seen that the values of  $k_D^{(LS)}$  for a-PMMA are positive for the seven samples

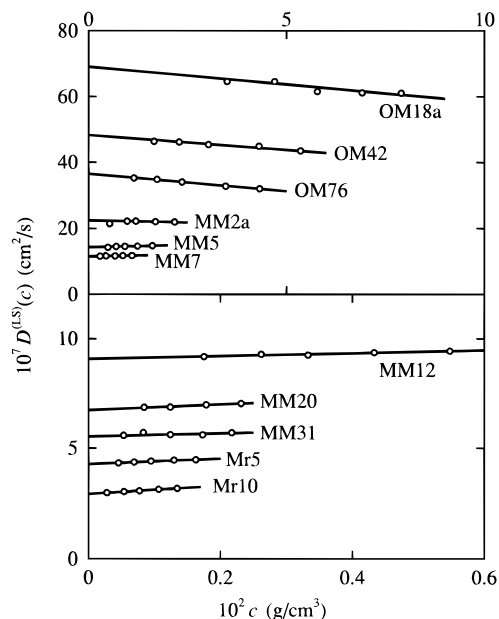


**Figure 1.** Plots of  $D^{(LS)}(c)$  against  $c$  for the a-PMMA samples indicated in acetone at 25.0 °C.

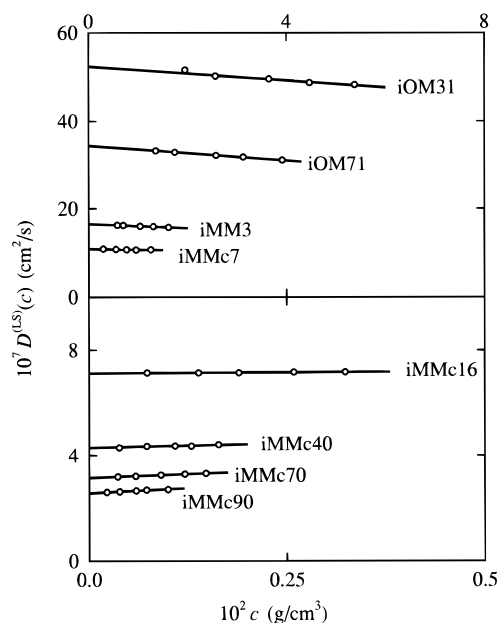


**Figure 2.** Plots of  $D^{(LS)}(c)$  against  $c$  for the i-PMMA samples indicated in acetone at 25.0 °C.

with the highest  $M_w$  and negative for the other four and that those for i-PMMA are positive for the four samples with the highest  $M_w$  and negative for the other four. Note that the values of  $k_D^{(LS)}$  are negative for all the samples of the two PMMA examined in acetonitrile, as already mentioned in the previous papers.<sup>16,17</sup>

The values of  $D$  and  $k_D^{(LS)}$  thus obtained for a- and i-PMMA in acetone at 25.0 °C are given in Tables 3 and 4, respectively, along with the present and previous<sup>16,17</sup> values in acetonitrile at the respective  $\Theta$ s. The tables also include the values of  $R_H$  and  $R_{H,\Theta}$  calculated from the defining equation

$$R_H = k_B T / 6\pi\eta_0 D \quad (1)$$

where  $k_B$  is the Boltzmann constant,  $T$  is the absolute temperature, and  $\eta_0$  is the viscosity coefficient of the solvent.

**Table 3. Results of DLS Measurements for Atactic Oligo- and Poly(methyl methacrylate)s**

sample	acetone, 25.0 °C			acetonitrile, 44.0 °C ( $\Theta$ )		
	$10^7 D$ , cm <sup>2</sup> /s	$k_D^{(LS)}$ , cm <sup>3</sup> /g	$R_H$ , Å	$10^7 D_\Theta$ , cm <sup>2</sup> /s	$k_D^{(LS)}$ , cm <sup>3</sup> /g	$R_{H,\Theta}$ , Å
OM18a	69.2	-1.6	10.3	78.0	-1.7	10.5
OM42	48.2	-1.8	14.8	57.5 <sup>a</sup>	-3.1 <sup>a</sup>	14.2
OM76	36.5	-2.9	19.6	40.8 <sup>a</sup>	-3.7 <sup>a</sup>	20.0
MM2a	22.4	-1.1	31.9	26.9	-6.1	30.3
MM5	14.3	1.8	49.9	17.6	-8.0	46.3
MM7	11.5	1.9	62.1	14.3 <sup>a</sup>	-11 <sup>a</sup>	57.0
MM12	9.07	7.4	78.8	11.6 <sup>a</sup>	-13 <sup>a</sup>	70.3
MM20	6.73	19	106	8.86	-16	92.0
MM31	5.53	13	129	7.32	-15	111
Mr5	4.29	29	166	5.88	-33	139
Mr10	2.93	64	244	4.19	-38	195

<sup>a</sup> The values of  $D_\Theta$  and  $k_D^{(LS)}$  have been reproduced from ref 16.

**Table 4. Results of DLS Measurements for Isotactic Oligo- and Poly(methyl methacrylate)s**

sample	acetone, 25.0 °C			acetonitrile, 28.0 °C ( $\Theta$ )		
	$10^7 D$ , cm <sup>2</sup> /s	$k_D^{(LS)}$ , cm <sup>3</sup> /g	$R_H$ , Å	$10^7 D_\Theta$ , cm <sup>2</sup> /s	$k_D^{(LS)}$ , cm <sup>3</sup> /g	$R_{H,\Theta}$ , Å
iOM31	52.4	-1.5	13.6	49.9 <sup>a</sup>	-2.6 <sup>a</sup>	13.4
iOM71	34.5	-2.5	20.7	33.0	-4.9	20.2
iMM3	16.6	-2.8	43.0	16.2	-9.8	41.1
iMMc7	10.9	-1.5	65.5	10.6	-14	62.9
iMMc16	7.12	2.3	100	7.16	-21	93.1
iMMc40	4.30	15	166	4.58	-36	146
iMMc70	3.15	37	227	3.40	-52	196
iMMc90	2.58	57	277	2.87	-66	232

<sup>a</sup> The values of  $D_\Theta$  and  $k_D^{(LS)}$  except for iMMc40 and iMMc70 have been reproduced from ref 17.

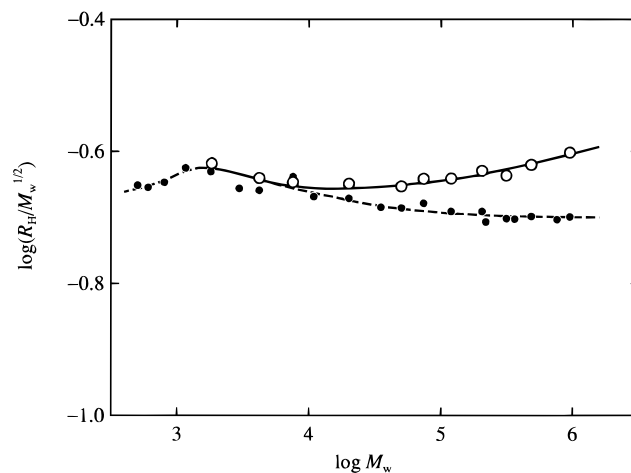


**Figure 3.** Double-logarithmic plots of  $R_H/M_w^{1/2}$  (in Å) against  $M_w$  for a-PMMA: (○) in acetone at 25.0 °C (present data); (●) in acetonitrile at 44.0 °C ( $\Theta$ ) (present and previous<sup>16</sup> data). The solid and dashed curves connect the data points smoothly.

Figures 3 and 4 show double-logarithmic plots of  $R_H/M_w^{1/2}$  (in Å) against  $M_w$  for a-PMMA (unfilled circles) and i-PMMA (unfilled triangles), respectively, in acetone at 25.0 °C. The present and previous<sup>16,17</sup> results for  $R_{H,\Theta}$  obtained for a-PMMA in acetonitrile at 44.0 °C ( $\Theta$ ) (filled circles) and for i-PMMA in acetonitrile at 28.0 °C ( $\Theta$ ) (filled triangles) are also plotted in Figures 3 and 4, respectively. (The previous result for  $R_{H,\Theta}$  for sample MM2a has been omitted here for the reason mentioned in the Experimental Section.) In each figure, the solid and dashed curves connect the data points smoothly (the latter for the solutions at  $\Theta$ ).

It is seen that for both a- and i-PMMA the difference between the values of  $R_H$  and  $R_{H,\Theta}$ , i.e., the excluded-

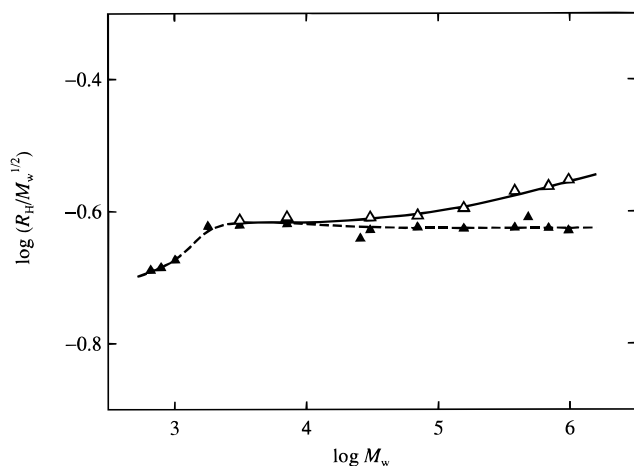


**Figure 4.** Double-logarithmic plots of  $R_H/M_w^{1/2}$  (in Å) against  $M_w$  for i-PMMA: (Δ) in acetone at 25.0 °C (present data); (▲) in acetonitrile at 28.0 °C (present and previous<sup>17</sup> data). The solid and dashed curves connect the data points smoothly.

**Table 5.** Values of  $\alpha_H$ ,  $\alpha_S$ , and  $\alpha_\eta$  for Atactic Oligo- and Poly(methyl methacrylate)s in Acetone at 25.0 °C

sample	$\alpha_H$	$\alpha_S$	$\alpha_\eta$
OM76	0.98	1.02 <sup>a</sup>	1.02 <sup>a</sup>
MM2a	1.05	1.05	1.04
MM5	1.08	1.14	1.08
MM7	1.09		1.10
MM12	1.12		1.11
MM20	1.15	1.21	1.15
MM31	1.16	1.25	1.18
Mr5	1.19	1.30	1.20
Mr10	1.25	1.38	1.26

<sup>a</sup> The values of  $\alpha_S$  and  $\alpha_\eta$  have been reproduced from ref 12 except for Mr10 (present work).

volume effect on  $R_H$  in acetone at 25.0 °C becomes appreciable for  $M_w \gtrsim 10^4$ . As was expected, the values of  $R_H$  for each PMMA agree with the corresponding values of  $R_{H,\Theta}$  in the oligomer region (for  $M_w \lesssim 10^4$ ) within experimental error. This agreement implies that the values of  $R_{H,0}$  for the unperturbed a- and i-PMMA chains in acetone at 25.0 °C may be considered to be identical with the corresponding values of  $R_{H,\Theta}$  in acetonitrile at the respective  $\Theta$ s. We may then evaluate  $\alpha_H$  correctly for both a- and i-PMMA in acetone by the use of the corresponding values of  $R_{H,\Theta}$  in acetonitrile as the respective reference standards.

**Mean-Square Radius of Gyration.** The values of  $\langle S^2 \rangle^{1/2}$  determined for sample Mr10 are 339 Å in acetone at 25.0 °C and 246 Å in acetonitrile at 44.0 °C (Θ). These values are used for the calculation of  $\alpha_S$  in the next section.

**Intrinsic Viscosity.** The values of  $[\eta]$  and the Huggins coefficient  $k'$  determined for sample Mr10 are 1.15 dL/g and 0.53, respectively, in acetone at 25.0 °C and 0.536 dL/g and -1.19, respectively, in acetonitrile at 44.0 °C (Θ). Those for sample iMMc7 in acetone at 25.0 °C are 0.300 dL/g and 0.48, respectively. These values of  $[\eta]$  and  $[\eta]_\Theta$  are used for the calculation of  $\alpha_\eta$  in the next section.

## Discussion

**Relations of  $\alpha_H$  to  $\alpha_S$  and  $\alpha_\eta$ .** In Table 5 are summarized the values of  $\alpha_H$  for all the a-PMMA samples in acetone at 25.0 °C calculated from the equation

$$R_H = R_{H,\Theta} \alpha_H \quad (2)$$

**Table 6.** Values of  $\alpha_H$ ,  $\alpha_S$ , and  $\alpha_\eta$  for Isotactic Oligo- and Poly(methyl methacrylate)s in Acetone at 25.0 °C

sample	$\alpha_H$	$\alpha_S$	$\alpha_\eta$
iOM71	1.02	1.01 <sup>a</sup>	1.02 <sup>a</sup>
iMM3	1.05	1.07	1.04
iMMc7	1.04		1.06
iMMc16	1.07		1.09
iMMc40	1.14	1.19	1.13
iMMc70	1.16	1.24	1.17
iMMc90	1.19	1.28	1.20

<sup>a</sup> The values of  $\alpha_S$  and  $\alpha_\eta$  have been calculated from the previous results<sup>9,13,17</sup> for  $\langle S^2 \rangle$ ,  $\langle S^2 \rangle_\Theta$ ,  $[\eta]$ , and  $[\eta]_\Theta$  except for  $[\eta]$  for iMMc7 (present work).

with the values of  $R_H$  and  $R_{H,\Theta}$  given in Table 3. The values of  $\alpha_S$  and  $\alpha_\eta$  in acetone at 25.0 °C given in Table 5 have been reproduced from ref 12 except for sample Mr10, for which the value of  $\alpha_S$  has been calculated from the equation

$$\langle S^2 \rangle = \langle S^2 \rangle_\Theta \alpha_S^2 \quad (3)$$

with the values of  $\langle S^2 \rangle^{1/2}$  and  $\langle S^2 \rangle_\Theta^{1/2}$  given in the Results section, and for which the value of  $\alpha_\eta$  has been calculated from the equation

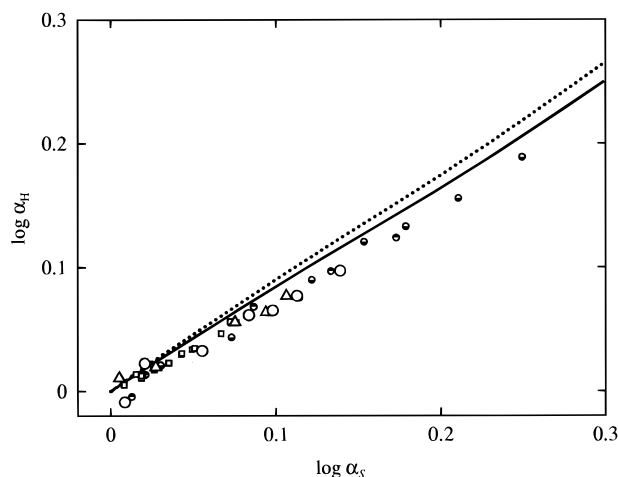
$$[\eta] = C_\eta [\eta]_\Theta \alpha_\eta^3 \quad (4)$$

with the values of  $[\eta]$  and  $[\eta]_\Theta$  given in the Results section and with  $C_\eta = 1.08$  as previously<sup>12</sup> determined.

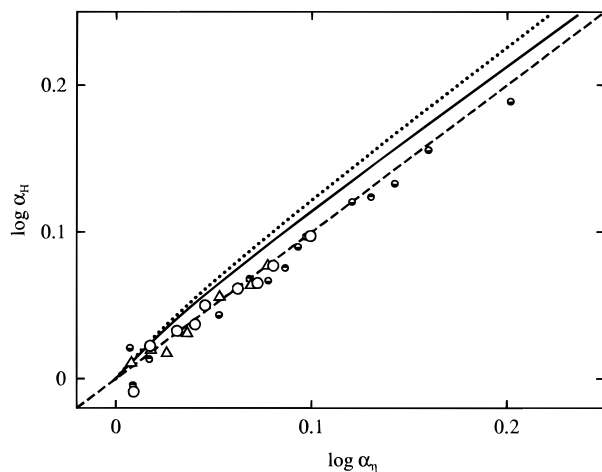
Similarly, in Table 6 are summarized the values of  $\alpha_H$  for all the i-PMMA samples in acetone at 25.0 °C calculated from eq 2 with the values of  $R_H$  and  $R_{H,\Theta}$  given in Table 4. The values of  $\alpha_S$  given in Table 6 have been calculated from eq 3 with the values of  $\langle S^2 \rangle^{1/2}$  in acetone at 25.0 °C given in Table 2 of ref 13 and those of  $\langle S^2 \rangle_\Theta^{1/2}$  in acetonitrile at 28.0 °C given in Tables 3 and 4 of ref 9 and in Table 3 of ref 13. The values of  $\alpha_\eta$  have been calculated from eq 4 with  $C_\eta = 1.04$  as previously<sup>13</sup> determined and with the values of  $[\eta]$  given in the Results section (for iMMc7) and in Table 4 of ref 13 and those of  $[\eta]_\Theta$  in acetonitrile at 28.0 °C given in Table 2 of ref 17.

Figure 5 shows double-logarithmic plots of  $\alpha_H$  against  $\alpha_S$  for a-PMMA (unfilled circles) and i-PMMA (triangles) in acetone at 25.0 °C. For comparison, it also includes the previous results for a-PS in toluene at 15.0 °C (bottom-half-filled circles),<sup>26</sup> in 4-*tert*-butyltoluene at 50.0 °C (top-half-filled circles),<sup>26</sup> and in cyclohexane at 36.0–45.0 °C (squares).<sup>27</sup> The dotted curve represents the values calculated from the Barrett equation<sup>28</sup> for  $\alpha_H$  and the Domb–Barrett equation<sup>29</sup> for  $\alpha_S$  (eqs 14 and 15 of ref 1, respectively). The solid curve represents the values calculated from the Yamakawa–Yoshizaki (YY) equation<sup>30</sup> for  $\alpha_H$  (eq 16 of ref 1), which takes account of the effect of fluctuating hydrodynamic interaction (HI) on the basis of the Gaussian chain, and eq 15 of ref 1 for  $\alpha_S$ .

From Figure 5, it is clearly seen that the present data points for a- and i-PMMA in acetone form a single composite curve together with those for a-PS. From these results together with those for PIB in the preceding paper,<sup>1</sup> we may conclude that  $\alpha_H$  becomes a function only of  $\alpha_S$  within experimental error irrespective of the differences in polymer species and solvent condition. All the data points are located definitely below the dotted curve, and even below the solid curve, so that it is reconfirmed that the Barrett equation and also the YY equation overestimate  $\alpha_H$ .



**Figure 5.** Double-logarithmic plots of  $\alpha_H$  against  $\alpha_S$ : (○) for a-PMMA in acetone at 25.0 °C (present data); (△) for i-PMMA in acetone at 25.0 °C (present data); (●) for a-PS in toluene at 15.0 °C (previous data);<sup>26</sup> (●) for a-PS in 4-*tert*-butyltoluene at 50.0 °C (previous data);<sup>26</sup> (□) for a-PS in cyclohexane at 36.0–45.0 °C (previous data).<sup>27</sup> The dotted and solid curves represent the values calculated from eqs 14 and 16 of ref 1 for  $\alpha_H$ , respectively, and eq 15 of ref 1 for  $\alpha_S$ .



**Figure 6.** Double-logarithmic plots of  $\alpha_H$  against  $\alpha_\eta$ . The symbols have the same meaning as in Figure 5. The dotted and solid curves represent the values calculated from eqs 14 and 16 of ref 1 for  $\alpha_H$ , respectively, and eq 19 of ref 1 for  $\alpha_\eta$ . The dashed line represents the relation  $\alpha_H = \alpha_\eta$ .

Next we examine the relation between  $\alpha_H$  and  $\alpha_\eta$ . The same data for  $\alpha_H$  as in Figure 5 except those for a-PS in cyclohexane are double-logarithmically plotted against  $\alpha_\eta$  in Figure 6. In the figure, the dashed straight line represents the relation  $\alpha_H = \alpha_\eta$ , and the dotted and solid curves represent the values calculated from eqs 14 and 16 of ref 1 for  $\alpha_H$ , respectively, and the Barrett equation<sup>31</sup> for  $\alpha_\eta$  (eq 19 of ref 1). As noted in the preceding paper,<sup>1</sup> the effect of fluctuating HI has been theoretically taken into account only for  $\alpha_H$  but not for  $\alpha_\eta$ .

As in Figure 5, the dotted curve in Figure 6 deviates significantly upward from the data points. The YY theoretical values of  $\alpha_H$  represented by the solid curve are seen to be closer to the observed ones but still larger than the latter. As in the cases of a-PS in toluene and in 4-*tert*-butyltoluene<sup>26</sup> and of PIB studied in the preceding paper,<sup>1</sup> it is found that the present data points also follow closely the dashed line, indicating that the relation  $\alpha_H = \alpha_\eta$  holds also for a- and i-PMMA in acetone.

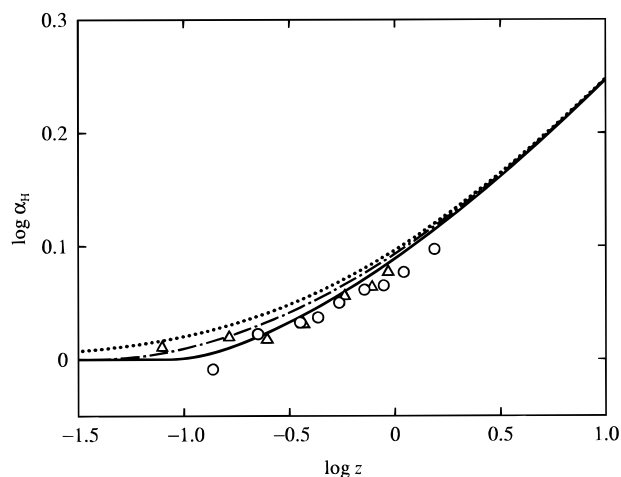


**Figure 7.** Double-logarithmic plots of  $\alpha_H$  against  $z$  for a- and i-PMMA in acetone at 25.0 °C. The symbols have the same meaning as in Figure 5. The solid and chain curves represent the values calculated from eq 16 of ref 1 with  $\tilde{z}$  in place of  $z$  for a- and i-PMMA, respectively, and the dotted curve represents the corresponding two-parameter-theory values (see text).

**$\alpha_H$  as Functions of  $z$  and  $\tilde{z}$ .** We examine the behavior of  $\alpha_H$  as functions of the conventional excluded-volume parameter  $z$  and of the scaled excluded-volume parameter  $\tilde{z}$  given by eqs 21 and 20 of ref 1, respectively.

Figure 7 shows double-logarithmic plots of  $\alpha_H$  against  $z$  for a-PMMA (unfilled circles) and i-PMMA (unfilled triangles) in acetone at 25.0 °C. Here, we have calculated their  $z$  values from eq 21 of ref 1 with the values of the parameters: the static stiffness parameter  $\lambda^{-1} = 57.9$  Å, the shift factor  $M_L = 36.3$  Å<sup>-1</sup>, and the reduced excluded-volume strength  $\lambda B = 0.22$  for a-PMMA and  $\lambda^{-1} = 38.0$  Å,  $M_L = 32.5$  Å<sup>-1</sup>, and  $\lambda B = 0.10$  for i-PMMA. Note that these values of  $\lambda^{-1}$  and  $M_L$  had been determined previously<sup>9,11</sup> from  $\langle S^2 \rangle_\Theta$ , and those of  $\lambda B$  from  $\alpha_S$ .<sup>12,13</sup> The solid and chain curves represent the values for a- and i-PMMA, respectively, calculated from eq 16 with eqs 14 and 15 of ref 1 with  $\tilde{z}$  in place of  $z$ , and the dotted curve represents the new YY two-parameter theory values calculated from eq 16 of ref 1 similarly (but with  $\tilde{z} = z$ ).

The solid and chain curves deviate downward progressively from the dotted curve with decreasing  $z$  (or decreasing  $M_w$ ) because of the effect of chain stiffness as in the case of  $\alpha_S$  and  $\alpha_\eta$ .<sup>12,13</sup> The effect remains rather large even for large  $z$  (or very large  $M_w$ ) and is more significant for a-PMMA than for i-PMMA (or for larger  $\lambda B$ ). The respective data points deviate remarkably downward from the dotted curve, and even from the solid and chain curves, over the whole range of  $z$  (or  $M_w$ ) studied. The implication is that the YY theory in the QTP scheme, which takes account of both effects of chain stiffness and fluctuating HI, still overestimates  $\alpha_H$  and may explain the observed results only semi-quantitatively.

Figure 8 shows double-logarithmic plots of  $\alpha_H$  against  $\tilde{z}$  with the same data as those in Figures 5–7. The light solid curve represents the values of  $\alpha_H$  calculated from eq 14 of ref 1, and the heavy solid curve represents those calculated from eq 16 with eqs 14 and 15 of ref 1, both with  $\tilde{z}$  in place of  $z$ . On the other hand, the dashed curve represents the values of  $\alpha_\eta$  calculated from eq 19 of ref 1 with  $\tilde{z}$  in place of  $z$ . It is seen that all the data points form a single composite curve, which may be identified with the dashed curve, over the whole range

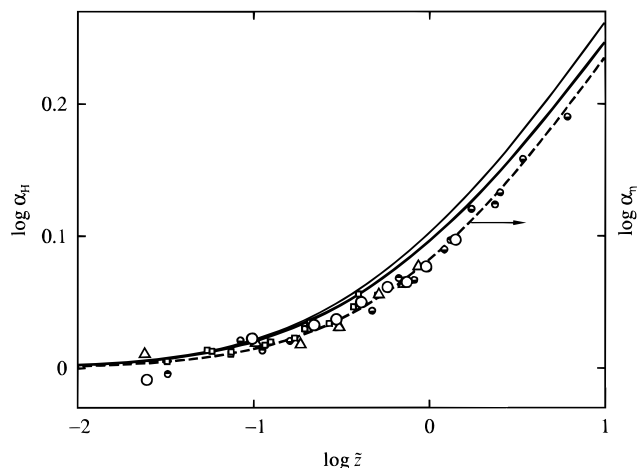


**Figure 8.** Double-logarithmic plots of  $\alpha_H$  against  $\tilde{z}$ . The symbols have the same meaning as in Figure 5. The light and heavy solid curves represent the values of  $\alpha_H$  calculated from eqs 14 and 16 of ref 1, respectively, with  $\tilde{z}$  in place of  $z$ . The dashed curve represents the values of  $\alpha_\eta$  calculated from eq 19 of ref 1 with  $\tilde{z}$  in place of  $z$ .

of  $M_w$  studied. From these results together with those for PIB in the preceding paper,<sup>1</sup> we may conclude that  $\alpha_H$  is a function only of  $\tilde{z}$  irrespective of the large differences in polymer species (chain stiffness and conformation) and solvent condition, or, in other words, the QTP scheme is valid for  $\alpha_H$  as well as for  $\alpha_S$  and  $\alpha_\eta$ .

As pointed out in the preceding paper<sup>1</sup> and also anticipated from the results in Figures 5 and 7, the light solid curve in Figure 8 deviates upward progressively from the data points with increasing  $\tilde{z}$ , and the deviation is decreased by taking account of the effect of fluctuating HI but cannot completely be explained by the YY equation, as shown by the heavy solid curve. It is evident that this incompleteness of the YY theory is due to its incomplete treatment of fluctuating HI itself, since the YSS theory (the QTP scheme) takes account of the effect of chain stiffness on the excluded-volume effect satisfactorily by the replacement of  $z$  by  $\tilde{z}$ .

## Conclusion

We have investigated the hydrodynamic-radius expansion factor  $\alpha_H$  as a function of the scaled excluded-volume parameter  $\tilde{z}$  (and also of  $\alpha_S$ ) for a-PMMA with  $f_r = 0.79$  and i-PMMA with  $f_r \approx 0.01$  in acetone at 25.0 °C. It has been found that for each PMMA the values of the hydrodynamic radius  $R_H$  in acetone agree with those of  $R_{H,\Theta}$  in acetonitrile at  $\Theta$  (i.e., 44.0 and 28.0 °C for a- and i-PMMA, respectively) in the oligomer region where the excluded-volume effect vanishes. Then, for both PMMAs, we have been able to determine  $\alpha_H$  by adopting the corresponding values of  $R_{H,\Theta}$  as the respective unperturbed values  $R_{H,0}$  in acetone at 25.0 °C.

In contrast to PIB studied in the preceding paper,<sup>1</sup> the effect of chain stiffness on  $\alpha_H$  is appreciable for both PMMAs as in the case of  $\alpha_S$  and  $\alpha_\eta$ .<sup>12,13</sup> Despite this fact, the present data points for  $\alpha_H$  as a function of  $\tilde{z}$  for them have been found to form a single composite curve together with the data for  $\alpha_H$  previously obtained for a-PS<sup>26,27</sup> and therefore also with those for PIB and poly(dimethylsiloxane)<sup>32</sup> within experimental error. Thus we may conclude that the QTP scheme (the YSS theory)

is valid for  $\alpha_H$  as well as for  $\alpha_S$  and  $\alpha_\eta$  irrespective of the large differences in chain stiffness, local conformation, and solvent condition.

As in the case of the other polymers,<sup>1,26,27,32</sup> it has been found that the experimental relation  $\alpha_H = \alpha_\eta$  holds also for the two PMMAs. Further, the Barrett equation has been again found to overestimate  $\alpha_H$ . This disagreement between theory and experiment may be explained only semiquantitatively by the Yamakawa–Yoshizaki theory, which takes account of the possible effect of fluctuating hydrodynamic interaction on  $\alpha_H$ . Therefore, their treatment of this effect is still incomplete, and it requires further theoretical investigations.

## References and Notes

- (1) Osa, M.; Abe, F.; Yoshizaki, T.; Einaga, Y.; Yamakawa, H. *Macromolecules* **1996**, *29*, 2302.
- (2) Abe, F.; Einaga, Y.; Yoshizaki, T.; Yamakawa, H. *Macromolecules* **1993**, *26*, 1884.
- (3) Yamakawa, H.; Stockmayer, W. H. *J. Chem. Phys.* **1972**, *57*, 2843.
- (4) Yamakawa, H.; Shimada, J. *J. Chem. Phys.* **1985**, *83*, 2607.
- (5) Shimada, J.; Yamakawa, H. *J. Chem. Phys.* **1986**, *85*, 591.
- (6) Yamakawa, H. *Annu. Rev. Phys. Chem.* **1984**, *35*, 23.
- (7) Yamakawa, H. In *Molecular Conformation and Dynamics of Macromolecules in Condensed Systems*; Nagasawa, M., Ed.; Elsevier: Amsterdam, 1988; p 21.
- (8) Yamakawa, H.; Shimada, J.; Fujii, M. *J. Chem. Phys.* **1978**, *68*, 2140.
- (9) Kamijo, M.; Sawatari, N.; Konishi, T.; Yoshizaki, T.; Yamakawa, H. *Macromolecules* **1994**, *27*, 5697.
- (10) Yamada, T.; Koyama, H.; Yoshizaki, T.; Einaga, Y.; Yamakawa, H. *Macromolecules* **1993**, *26*, 2566.
- (11) Tamai, Y.; Konishi, T.; Einaga, Y.; Fujii, M.; Yamakawa, H. *Macromolecules* **1990**, *23*, 4067.
- (12) Abe, F.; Horita, K.; Einaga, Y.; Yamakawa, H. *Macromolecules* **1994**, *27*, 725.
- (13) Kamijo, M.; Abe, F.; Einaga, Y.; Yamakawa, H. *Macromolecules* **1995**, *28*, 1095.
- (14) Fujii, Y.; Tamai, Y.; Konishi, T.; Yamakawa, H. *Macromolecules* **1991**, *24*, 1608.
- (15) Konishi, T.; Yoshizaki, T.; Yamakawa, H. *Macromolecules* **1991**, *24*, 5614.
- (16) Dehara, K.; Yoshizaki, T.; Yamakawa, H. *Macromolecules* **1993**, *26*, 5137.
- (17) Sawatari, N.; Konishi, T.; Yoshizaki, T.; Yamakawa, H. *Macromolecules* **1995**, *28*, 1089.
- (18) Takaeda, Y.; Yoshizaki, T.; Yamakawa, H. *Macromolecules* **1993**, *26*, 3742.
- (19) Takaeda, Y.; Yoshizaki, T.; Yamakawa, H. *Macromolecules* **1995**, *28*, 4167.
- (20) Yoshizaki, T.; Hayashi, H.; Yamakawa, H. *Macromolecules* **1993**, *26*, 4037.
- (21) Horita, K.; Yoshizaki, T.; Hayashi, H.; Yamakawa, H. *Macromolecules* **1994**, *27*, 6492.
- (22) Abe, F.; Einaga, Y.; Yamakawa, H. *Macromolecules* **1994**, *27*, 3262.
- (23) Abe, F.; Einaga, Y.; Yamakawa, H. *Macromolecules* **1995**, *28*, 694.
- (24) Kamijo, M.; Abe, F.; Einaga, Y.; Yamakawa, H. *Macromolecules* **1995**, *28*, 4159.
- (25) Takaeda, Y.; Yoshizaki, T.; Yamakawa, H. *Macromolecules* **1995**, *28*, 682.
- (26) Arai, T.; Abe, F.; Yoshizaki, T.; Einaga, Y.; Yamakawa, H. *Macromolecules* **1995**, *28*, 3609.
- (27) Arai, T.; Abe, F.; Yoshizaki, T.; Einaga, Y.; Yamakawa, H. *Macromolecules* **1995**, *28*, 5458.
- (28) Barrett, A. J. *Macromolecules* **1984**, *17*, 1561.
- (29) Domb, C.; Barrett, A. J. *Polymer* **1976**, *17*, 179.
- (30) Yamakawa, H.; Yoshizaki, T. *Macromolecules* **1995**, *28*, 3604.
- (31) Barrett, A. J. *Macromolecules* **1984**, *17*, 1566.
- (32) Horita, K.; Sawatari, N.; Yoshizaki, T.; Einaga, Y.; Yamakawa, H. *Macromolecules* **1995**, *28*, 4455.

MA951274N